



Photoemission calculations of metals W and Be

Lalthakimi Zadeng

Department of Physics, Mizoram University, Aizawl, Mizoram

Received 23 November 2014 | Revised 7 December 2014 | Accepted 13 December 2014

ABSTRACT

Photocurrents were calculated using initial state wavefunction obtained by solving one dimensional Schrödinger equation in terms of Greens function where the crystal potential is defined by Kronig-Penny δ -potential. Also a spatially dependent vector potential is used. This model is applied to the case of metals W and Be.

Key words: Green function; photoemission; photocurrent; vector potential.

INTRODUCTION

Angle-resolved photoemission technique is now one of the most widely used experimental tools for studying the band structure in simple and complex systems. Several mathematical models have been developed to interpret the experimental photoemission results. In photoemission, the evaluation of the matrix element $\langle \Psi_f | H' | \Psi_i \rangle$ is of prime importance as it is directly involved in the photocurrent density formula as given by Fermi golden rule.¹ However the presence of the surface poses a serious problem as the calculation of the initial state wavefunction Ψ_i is a complicated problem and is of fundamental importance also.

Photocurrent calculations using the initial state wavefunction Ψ_i deduced by Green func-

tion's method by solving Schrödinger equation² is presented in this paper. The crystal potential is defined by Kronig-Penny model to obtain Ψ_i . For the surface state photoemission, Ψ_i is described by the normalized Gaussian state wavefunction whose location with respect to the nominal surface plane is determined by z_0 . The photocurrent is calculated by incorporating the spatially dependent vector potential which is a modified form of the dielectric model as used by Bagchi and Kar.³

FORMALISM

The photocurrent density formula from golden rule¹ approximation can be written as

$$\frac{dj(E)}{d\Omega} = \frac{2\pi}{\hbar} \sum |\langle \psi_f | H' | \psi_i \rangle|^2 \delta(E - E_f),$$

$$\delta(E_f - E_i - \hbar\omega) f_o(E - \hbar\omega) [1 - f_o(E)] \quad (1)$$

Corresponding author: Zadeng

Phone:

E-mail: kimizadeng@gmail.com

where ψ_i (ψ_f) refer to the initial (final) state wavefunctions and the perturbation H' can be written as

$$H' = \left(\frac{e}{2mc}\right)(\mathbf{A} \cdot \mathbf{p} + \mathbf{p} \cdot \mathbf{A}) \quad (2)$$

where m is the mass of the electron, \mathbf{p} the one-electron momentum operator and \mathbf{A} the vector potential of the incident photon field.

The photon field vector formulae used in our calculations is obtained by using the dielectric model of Bagchi and Kar³. With simple modifications, we can write the photon field vector as

$$\tilde{A}_\omega(z) = \begin{cases} A_1, & z \leq -a \text{ (Bulk)} \\ \frac{A_1 a \varepsilon(\omega)}{[1-\varepsilon(\omega)]z+a}, & -a \leq z \leq 0 \text{ (Surface)} \\ A_1 \varepsilon(\omega), & z \geq 0 \text{ (Vacuum)} \end{cases} \quad (3)$$

where $A_1 = -\frac{\sin 2\theta_i}{[\varepsilon(\omega) - \sin^2 \theta_i]^{1/2} + \varepsilon(\omega) \cos \theta_i}$ is

a constant depending on the dielectric function $\varepsilon(\omega)$ photon energy $\hbar\omega$ and angle of incidence θ_i .

The initial state wavefunction deduced by using Green's function method is given by

$$\psi_i(z) = \begin{cases} \frac{-4\pi p C \sin^2 k_i a}{k_i a (k_i \cos k_i a + k_i - \chi \sin k_i a) \left(1 + e^{-ik_i a}\right) (1 + \cos k_i a)} \{k_i \cos k_i z - \chi \sin k_i z\} e^{-\mu z} & z < 0 \\ \frac{-4\pi p C \sin^2 k_i a}{k_i a (k_i \cos k_i a + k_i - \chi \sin k_i a) \left(1 + e^{-ik_i a}\right) (1 + \cos k_i a)} k_i e^{-\chi z} & z > 0 \end{cases} \quad (4)$$

where $C = \left(\frac{m_e}{2\pi k_i}\right)^{1/2}$, $k = \pm \frac{\pi}{a}$, $k_i^2 = \frac{2mE_i}{\hbar^2}$, $\chi^2 = \frac{2m}{\hbar^2}(V_0 - E_i)$, $\mu = k_i - \pi/d$.

In Eq. 4, for the surface state photoemission calculations, $\psi_i(z)$ is replaced by a properly normalized Gaussian form of the wavefunction located at $z = z_0$ plane and is given by

$$\Psi_i(z) = (2\beta/\pi a^2)^{1/4} \exp[-\beta(z - z_0)^2/a^2] \quad (5)$$

where β describes the width of the Gaussian and is a dimensionless quantity, a is the surface width.

The final state wavefunction ψ_f is the scattering state due to the existence of a step potential at the surface plane $z = 0$. This potential is defined by $V(z) = -V_0 \theta(z)$, where $\theta(z)$ is a unit function. Therefore ψ_f is given by

$$\psi_f(z) = \begin{cases} \left(\frac{m}{2\pi\hbar^2 k_f} \right)^{\frac{1}{2}} \frac{2k_f}{q_f + k_f} e^{ik_f z} e^{-\alpha|z|}, & z < 0 \quad (\text{bulk \& surface}) \\ \left(\frac{m}{2\pi\hbar^2 k_f} \right)^{\frac{1}{2}} \left(e^{ik_f z} + \frac{k_f - q_f}{q_f + k_f} e^{-ik_f z} \right), & z > 0 \quad (\text{vacuum}) \end{cases}$$

where $k_f^2 = \frac{2mE_f}{\hbar^2}$ and

$$q^2 = \frac{2m}{\hbar^2}(E_f - V_0) \text{ and } E_f = E_i + \hbar\omega.$$

The factor $e^{-\alpha|z|}$ is included on the bulk to take into account the inelastic scattering of the electrons. The photocurrent was calculated by evaluating the matrix element in Eq. (1) and by using the above wavefunctions in Eqs. (4), (5) and (6).

The matrix element when expanded is given by

$$\begin{aligned} I &= \langle \psi_f | \tilde{A}_\omega(z) \frac{d}{dz} + \frac{1}{2} \frac{d}{dz} \tilde{A}_\omega(z) | \psi_i \rangle \\ &= \int_{-\infty}^{-a} \psi_f^* \tilde{A}_\omega \psi_i dz + \int_{-a}^0 \psi_f^* \tilde{A}_\omega \frac{d\psi_i}{dz} dz \\ &\quad + \frac{1}{2} \int_{-a}^0 \psi_f^* \frac{d\tilde{A}_\omega}{dz} \psi_i dz + \int_0^\infty \psi_f^* \tilde{A}_\omega \frac{d\psi_i}{dz} dz \end{aligned}$$

Some of the matrix element could not be solved analytically, hence FORTRAN programs were written to solve it. Using the same model and parameters as above, photocurrents were calculated for W and Be but with the Fresnel field which is given by

$$\tilde{A}_\omega(z) = \begin{cases} - \frac{\sin 2\theta_i}{[\varepsilon(\omega) - \sin^2 \theta_i]^{1/2} + \varepsilon(\omega) \cos \theta_i}, & z < 0 \quad (\text{Bulk \& Surface}) \\ - \frac{\sin 2\theta_i}{[\varepsilon(\omega) - \sin^2 \theta_i]^{1/2} + \varepsilon(\omega) \cos \theta_i} \varepsilon(\omega), & z > 0 \quad (\text{Vacuum}) \end{cases} \quad (7)$$

This was done in order to see the effect inclusion of surface width in our model.

RESULTS AND DISCUSSIONS

The model developed is used to calculate photocurrents from metals W and Be. As it is a model calculation, the following data is used for all the case. Height of the potential barrier $V_o=15\text{eV}$, Scattering factor $\alpha=0.5$, Lattice constant, $a = 5.29 \text{ \AA}$, Initial state energy $E_i = 10\text{eV}$ and width of the Gaussian form of wavefunction $\beta=1$.

Photocurrent was calculated as a function of photon energy $\hbar\omega$ for the location of the initial state wavefunction ψ_i at different values of z_o and for the same values of the surface width given by $a = 5.29 \text{ \AA}$. In Fig. 1, we show the variation of photocurrent plotted against photon energy ($\hbar\omega$) for values of $z_o = 0, - 2.645$ and $- 5.29 \text{ \AA}$ for W. We find that for $z_o = - 2.645 \text{ \AA}$, the photocurrent increases with the increase of $\hbar\omega$ and becomes maximum at $\hbar\omega = 20 \text{ eV}$. With the further increase of photon energy, photocurrent decreases and shows a minimum value at $\hbar\omega = 26 \text{ eV}$. The bulk plasmon energy

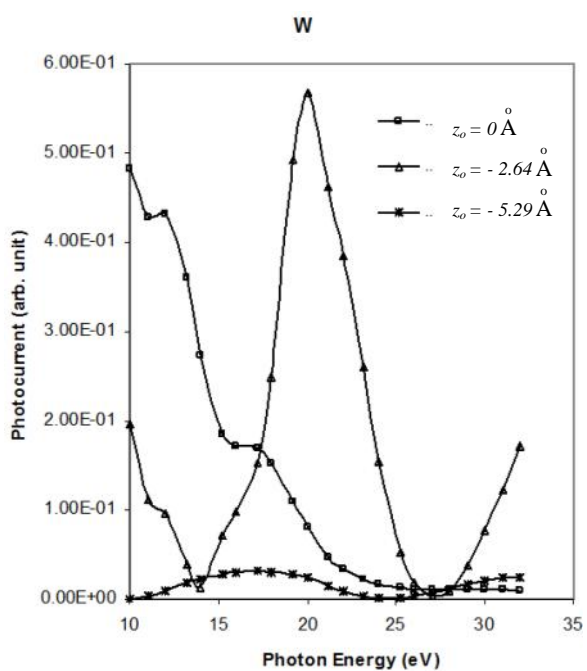


Figure 1.

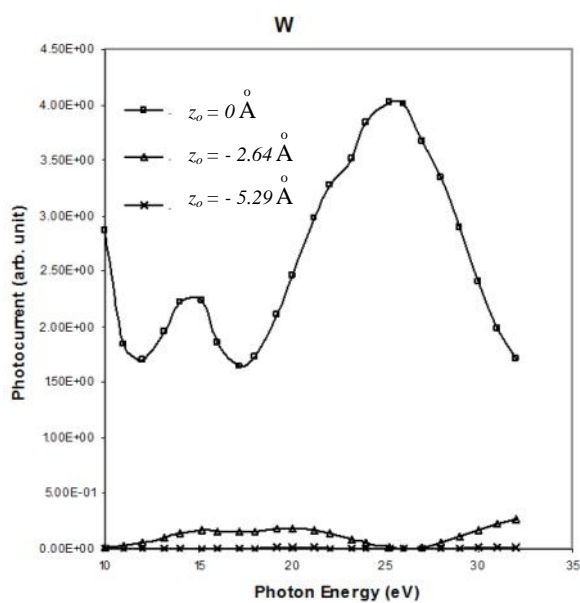


Figure 2.

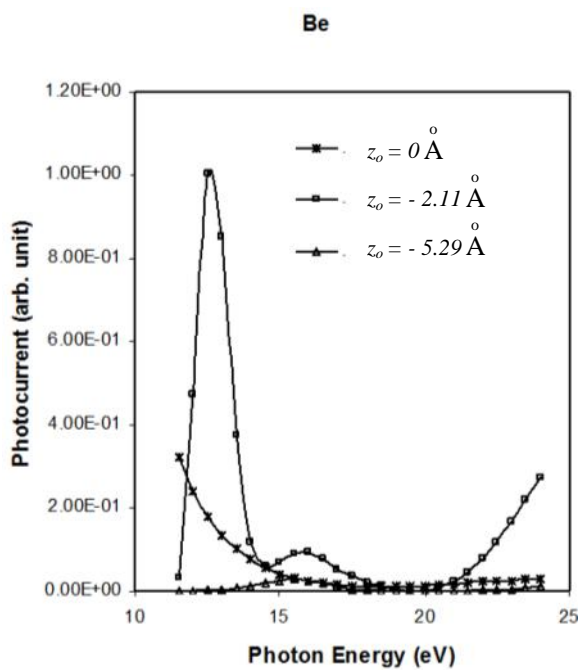


Figure 3.

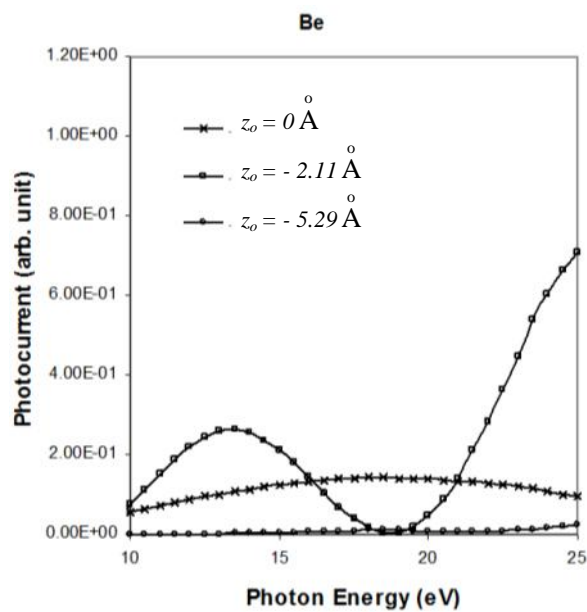


Figure 4.

($\hbar\omega_p$) of W is 25 eV. This means that photocurrent tends towards a minimum as $\hbar\omega$ tends to $\hbar\omega_p$.

We have seen that such features are also present in the experimentally observed results of Weng *et al.*⁴ in which the minimum occurs at $\hbar\omega = 25\text{ eV}$ and also the theoretical calculation of Bagchi and Kar³. For the other two locations of the initial state wavefunction ψ_i , that is, $z_0 = 0$ and -5.29 \AA , this kind of feature as obtained in the case of $z_0 = -2.645\text{ \AA}$ is not exhibited. Although a minimum is shown at around $\hbar\omega = \hbar\omega_p$, peak in photocurrent below $\hbar\omega_p$ is not obtained. Fig. 2 shows the plot of photocurrent against photon energy from W with the inclusion of Fresnel fields as shown in Eq. (13) for $z_0 = 0, -2.645$ and -5.29 \AA . In this case we have observed that for the location of initial state wavefunction ψ_i at $z_0 = -2.645\text{ \AA}$, there is no peak in photocurrent at $\hbar\omega = 20\text{ eV}$ that is, below the plasmon energy. There is essentially no peak in photocurrent at all although an occurrence of minimum is shown at $\hbar\omega = \hbar\omega_p$. For $z_0 = 0\text{ \AA}$, the plot showed a maximum but at $\hbar\omega = \hbar\omega_p$ the plasmon energy of W.

In Fig. 3, we have a plot of photocurrent against photon energy ($\hbar\omega$) for values of $z_0 = 0, -2.116$ and -5.29 \AA in the case of Be. We find that for $z_0 = -2.116\text{ \AA}$, the photocurrent increases with the increase of $\hbar\omega$ and becomes maximum at $\hbar\omega = 12\text{ eV}$, the photocurrent then decreases and a minimum is observed at $\hbar\omega = 14\text{ eV}$. With further increase in photon energy, a second hump in photocurrent is observed at $\hbar\omega = 16\text{ eV}$, and a second minimum at $\hbar\omega = 19\text{ eV}$. The plasmon energy ($\hbar\omega_p$) of Be is 19.9 eV⁵. The results of photocurrent shown in Fig. 3 for location of ψ_i at $z_0 = -2.116\text{ \AA}$ showed similar behavior as that obtained experimentally by Bartynski *et al.*⁶ This is similar to calculated

results of Thapa and Kar⁷. For the other two locations of ψ_i , that is, $z_0 = 0$ and -5.29 \AA , we do not observe such kind of features. Fig.4 shows the plot of photocurrent against photon energy from Be with the inclusion of Fresnel fields for the location of ψ_i at $z_0 = 0, -2.116$ and -5.29 \AA . For the location of initial state wavefunction ψ_i at $z_0 = -2.116\text{ \AA}$, there is occurrence of a small hump in photocurrent at $\hbar\omega = 12\text{ eV}$ followed by a minimum at $\hbar\omega = 19\text{ eV}$, with the increase of the photon energy, the photocurrent increases sharply. For the location of ψ_i at $z_0 = 0$ and -5.29 \AA , there are essentially no maximum and minimum on photocurrent.

CONCLUSION

In this model, the calculation of the initial state wavefunction ψ_i by Green function's method was considered only for the bulk photoemission. For the surface we have assumed the initial state wavefunction to be a Gaussian type of wavefunction. The model presented here reproduces results as obtained by other theoretical models like free electron model of Thapa,⁸ Kronig Penny potential model of Thapa⁹ and Mathieu potential model of Pachuau.¹⁰ Hence, from the above observations we can conclude that though our model is obtained by simple calculations it works well and is applicable to metals such as W and Be.

REFERENCES

1. Penn DR (1972). Photoemission spectroscopy in the presence of adsorbate-covered surfaces. *Phys Rev Lett*, **28**, 1041.
2. Davison SG & Steslicka M (1992). *Basic Theory of Surface States*, Oxford.
3. Bagchi A & Kar N (1978). Refraction effects in angle-resolved photoemission from surface states on metals. *Phys Rev B* **18**, 5240-5247.
4. Weng SL, Gustafsson T & Plummer EW (1977). Three surface resonances on the (100) face of W and Mo: an

- angle-resolved synchrotron photoemission study. *Phys Rev Letts*, **39**, 822-825.
5. Klemperer O & Shepherd JPG (1963). Characteristic energy losses of electrons in solids. *Adv Phys*, **17**, 335.
 6. Bartynski RA, Jensen E, Gustafsson T & Plummer EW (1985). Angle-resolved photoemission investigation of the electronic structure of Be: Surface states. *Phys Rev B* **32**, 952.
 7. Thapa RK & Kar N (1995). Photocurrent calculations in beryllium using a local dielectric model. *Phys Rev B*, **49**, 17980.
 8. Das P, Thapa RK & Kar N (1991). Photoemission calculation with a simple model for the photon field: application to aluminium. *Mod Phys Lett B* **5**, 65–72.
 9. Thapa RK & Kar N (1988). Photoemission calculation from band states using Kronig-Penney model and spatially varying photon field. *Ind Jour Pure Appl Phys*, **26**, 620-623.
 10. Pachuau Z, Zoliana B, Patra PK, Khating DT & Thapa RK (2002). Application of Mathieu potential to photoemission calculations: the case of a strong potential. *Phys Letts A*, **294**, 52.